UDK 612.063:616.8:616.12-009.72
Original scientific article/Izvirni znanstveni članek

ISSN 1580-2949
MTAEC9, 55(3)387(2021)

SHORT-TERM EFFECTS OF SELECTIVE TRANSCUTANEOUS AURICULAR-NERVE STIMULATION MEASURED IN A SUBJECT WITH ANGINA PECTORIS

KRATKOTRAJNI UČINKI TRANSKUTANE ELEKTRIČNE STIMULACIJE AVRIKULARNEGA ŽIVCA PRI OSEBI Z ANGINO PEKTORIS

Janez Rozman[1,3*], Larisa Stojanovic[2], Samo Ribarič[3]

[1]Center for Implantable Technology and Sensors, ITIS d. o. o. Ljubljana, Lepi pot 11, 1000 Ljubljana, Republic of Slovenia
[2]Institute of Anatomy, Faculty of Medicine, University of Ljubljana, Korytkova 2, 1000 Ljubljana, Republic of Slovenia
[3]Institute of Pathophysiology, Faculty of Medicine, University of Ljubljana, Zaloška 4, 1000 Ljubljana, Republic of Slovenia

Prejem rokopisa – received: 2020-01-04; sprejem za objavo – accepted for publication: 2021-02-25

doi:10.17222/mit.2021.011

We have measured the short-term effects of selective, transcutaneous, auricular-nerve stimulation (tANS) on the heart function, respiratory function, thermal function and galvanic skin response in a patient with angina pectoris with respect to four predefined sites on the left and right cymba concae (CC). The tANS involved the use of a train of monopolar, current, biphasic pulses composed of rectangular cathodic i_c and anodic phases i_a and globule-like platinum stimulating electrodes. The parameters of the stimulating pulses were as follows: frequency f = 45.5 Hz, cathodic phase width t_c = 200 μs, anodic phase width t_a = 200 μs, interphase delay d = 180 μs, pulse-train duration 2.0 s and time gap between pulse trains 1.0 s. The results show that tANS at predefined sites on the CC produce measurable effects on the assessed vital functions. In conclusion, tANS with an increased number of channels, has the potential to be used in the treatment of certain disorders.

Keywords: transcutaneous auricular-nerve stimulation, external ear, platinum electrodes, stimulating pulse, physiological measurements.

Merili smo kratkoročne učinke selektivne transkutane stimulacije avrikularnega živca (tANS) na funkcijo srca, funkcijo dihanja, termično funkcijo in na prevodnost kože pri pacientu z angino pectoris, izvedene na štirih prednastavljenih mestih levega in desnega zunanjega ušesa (CC). Za tANS smo uporabili vlake monopolarnih, tokovnih, izmeničnih pulzov sestavljenih iz pravokotne katodne faze i_c, anodne faze i_a in platinastih stimulacijskih elektrod v obliki kroglice. Parametri stimulacijskih pulzov so bili naslednji: frekvenca f = 45,5 Hz, dolžina katodne faze t_c = 200 μs, dolžina anodne faze t_a = 200 μs, časovni zamik med fazama d =180 μs, dolžina vlaka 2 s in pavza med vlaki impulzov 1 s. Rezultati kažejo, da tANS prednastavljenih mest na CC povzroči merljive učinke na merjene življenjske funkcije. Zaključimo lahko, da bi bilo mogoče tANS ob povečanem številu kanalov uporabiti pri obravnavi določenih zdravstvenih težav.

Ključne besede: transkutana električna stimulacija avrikularnega živca, zunanje uho, platinaste elektrode, stimulacijski impulz, fiziološke meritve

1 INTRODUCTION

Functional nerve stimulation that modulates the activity patterns on peripheral nerves is a novel way of treating diverse medical conditions, such as nervous-system disorders like epilepsy, refractory depression and chronic obesity. Therapies like invasive vagus nerve stimulation (VNS)[1–4] and tANS[5] have been proposed. However, unlike cervically implanted VNS, tANS is a non-invasive method that is able to modulate the vagus system. Rapid developments in basic research mean that tANS could serves as a safe, inexpensive and transportable neurostimulation system for the treatment of some central and peripheral diseases.[6] tANS is actually a combined diagnostic and treatment system based on normalizing the body's dysfunction through the stimulation of the auricular branch of the vagus nerve, thereby delivering an electrical stimulation to specific sites on the external ear.[7–10] The external ear has been chosen, because it is the only place on the surface of the human body where there is a dense distribution of afferent vagus nerve fibres and receptors, such as nociceptors, Golgi-tendon receptors, Meissner corpuscles, Krause's end-bulbs and glomus bodies.[11]

Accurate thermometry of the skin is an important physiological measurement that can provide us with an insight into the localised interactions between the autonomic nervous system and human physiology.[12,13] This is because heat exchanges at the surface of the skin can both contribute to and challenge thermal homeostasis. In the past, skin temperature was measured with various devices that were affixed to the skin.[14] Although such devices have improved recently, accurate measurements of the skin-surface temperature remain difficult to realise.[15] One of the reasons for this is that contact sensors are applied to the surface of the skin, so preventing the evapo-

*Corresponding author's e-mail:
janez.rozman@guest.arnes.si

ration of sweat, and so leading to the area under the sensor having a higher temperature than other points on the skin.[16] As a result, infrared (IR) devices are increasingly being utilised for measurements of skin temperature. IR is an invisible form of light that has a wavelength from 0.65 μm to 20 μm. Humans emit very-long-wavelength IR because they are warm.[17] Measurements of the temperature provide an average based on the amount of IR energy emitted by the area of skin in front of the thermometer.

Normal body temperature (BT) for an adult is around 37 °C. However, an individual's normal baseline body temperature can be 0.6 °C higher or lower, depending on the person's activity and the time of the day. The temperature can be measured at many places on the body, for example, the mouth (oral method), anus (rectal method), armpit (axillary method), or ear (tympanic method). The rectal temperature is 0.3 °C to 0.6 °C higher than the oral temperature. Similarly, the tympanic temperature is up to 0.6 °C higher than the oral temperature. The temperature in the armpit is usually lower by 0.3 °C to 0.6 °C than the oral temperature, as is the forehead (temporal) temperature[18] measured with a scanner. The most accurate way to measure body temperature is to take a rectal reading. Being aware of these differences is important when evaluating subtle variations in the skin's temperature associated with tANS, which could highlight some important interactions between the autonomic nervous system and human physiology.[19]

The thyroid is a butterfly-shaped endocrine gland in the neck. It consists of a left and a right lobe, connected by a narrow isthmus that lies anterior to rings 2 to 4 of the trachea. Each lobe is about 5 cm long, 3 cm wide and 2 cm thick, and the isthmus is about 1.25 cm in height and width. The thyroid is highly vascular and receives a greater flow of blood than most other tissues in the body.[20] The thyroid is responsible for the production of the thyroid hormones thyroxine (T4) and triiodothyronine (T3). They are important for the metabolic functions of many major organs, including the heart, brain, liver, and muscles. Various factors such as acute illness, coexisting morbidities, and certain medications can affect the thyroid's synthesis of hormones.[21]

It is well known that a low BT is one of the major clinical signs of possible thyroid or adrenal dysfunction. Accordingly, when thyroid hormone expression is dysregulated, the temperature of the body is altered.[22] For hyperthyroidism the assessed temperature would be above 37 °C and in hypothyroidism, less than 36.55 °C. Therefore, thermography could be used during the clinical diagnosis of thyroid diseases.[23]

The thyroid is dually innervated by sympathetic and parasympathetic nerve fibres.[24] The parasympathetic nerve fibres come from the vagus nerves, i.e., the superior laryngeal nerve and the recurrent laryngeal nerve, while sympathetic nerve fibres come from the superior, middle and inferior cervical ganglia of the sympathetic trunk.[24] Hotta et al.,[25] examined the effects of the electrical stimulation of efferent or afferent nerve fibres innervating the thyroid on the secretion of T3 and T4 from the thyroid in anesthetized and artificially ventilated rats. The secretion of T3 and T4 increased during superior laryngeal nerve stimulation and decreased during inferior cervical ganglia of the sympathetic trunk stimulation. Furthermore, Ishii et al.,[26] showed that VNS accelerated the secretion of thyroid hormones by increasing the blood-flow rate and its hormone concentration in the thyroid venous blood.

The effectiveness of various forms of tVNS for heart-related conditions has not been investigated beyond several pilot studies. Related investigations showed that the vagal tone elicited by auricular acupuncture or auricular acupressure typically leads to a reduction in the HR and blood pressure (BP) in vascular hypertensive patients,[27] while in healthy volunteers it leads to a significant decrease in the HR and a significant increase in the HR's variability.

Galvanic skin response (GSR) is a method of measuring the electrical conductance of the skin. It is commonly used as a very precise stress indicator. The device is essentially an ohmmeter that measures the electrical conductance between two sites. This is of interest because the sweat glands are controlled by the autonomous nervous system, so tANS supposedly changes the electrical conductance of the skin and thus the state of relaxation or stress.

The key indicators for the state of a person's health are HR, BP, BT and breathing rate (BR). An additional, and important, indicator is pulse oximetry. SpO2 or arterial haemoglobin saturation is defined as a measure of the amount of oxygen dissolved in the blood, based on the detection of oxygenated and de-oxygenated haemoglobin. It is expressed as a percentage of complete saturation. In other words, SpO2 is the ratio of the amount of oxygen bound to the haemoglobin to the oxygen-carrying capacity of the haemoglobin.[28] Besides being a non-invasive measurement of SpO2, pulse oximeters often provide a patient's HR via an assessment of the arterial blood pulsations (BPU). Pulse oximeters are able to visualize a blood-volume change in the tissue caused by the passage of blood, and this is called a plethysmographic trace (PLW). A PLW can resemble an arterial pressure waveform and is approximated by the ratio of the stroke volume output to the compliance of the arterial tree. With each beat of the heart, the compliance of the arterial tree reduces the BPU to almost zero in the capillaries, thus making tissue blood flow mainly continuous and with very little pulsation.

Few studies to date have quantified the inter-individual variability of nasal airflow. The review of Eccles,[29] examined the basic scientific and clinical knowledge that is essential for a proper understanding of the usefulness of measurements of nasal airflow in clinical practice. Namely, the afferent nerves in the airways serve to regu-

late breathing patterns, cough, and airway autonomic neural tone. tANS that potentially influences afferent nerve activity can act directly on the nerve fibres and thus alters the airway physiology. More recently, Borojeni et al.,[30] reported normative ranges of nasal airflow variables in healthy adults. They found that the lower limit of normative unilateral airflow is (60 ± 20) mL/s, whereas the upper limit of normative unilateral airflow is (191±20) mL/s. To measure the trans-nasal airflow proximal to the patient, a nasal flowmeter is normally used.[31] It provides valuable data from the airway opening, and the whole ventilation process depends on these measurements and their accuracy. Correct volume, airflow, and pressure data make it possible to better assess a patient's respiratory function and lung condition.

The selectivity of all the tANS modalities, however, is exclusively dependent on the localized electric charge delivered to specific populations of receptors, so the applications require electrodes with a high spatial selectivity, a low impedance, and a safe reversible charge injection for the tANS.[32]

This study aims to investigate the effects of selective tANS at predefined sites for both cymba concae (CC) on some vital functions of a 62-year-old patient with stable angina pectoris 6 years after an acute myocardial infarction. These vital functions are as follows: respiratory function, thermal function, physiological arousal and heart function. With regard to the respiratory function, the aim was to measure BR, breath length (LBR), peak-to-peak air flow (AFBR), maximum slope of air flow (SBR) and SpO2, assuming that they could be altered with the tANS. With regard to thermal function, the aim was to measure the skin's temperature of the left lobe (TLL), the right lobe (TRL) of the thyroid and the BT,[33] assuming that they can be altered with the tANS.

With regard to physiological arousal, the aim was to measure the GSR, assuming that it can be altered with the tANS. With regard to the heart function, the aim was to measure the HR, the length of blood pulsations during inhalation (LBPUINH), the length of blood pulsations during exhalation (LBPUEXH), the peak-to-peak plethysmographic trace of the blood pulsations during inhalation (PLWINH) and the peak-to-peak plethysmographic trace of the blood pulsations during exhalation (PLWEXH), assuming that all can be altered with the tANS. One specific aim was to assess the effect of the tANS on the interaction of the ventilation and circulation using a calculation of the dynamic viscosity during inhalations (DVINH) and the dynamic viscosity during exhalations (DVEXH), respectively.

2 EXPERIMENTAL PART

The experimental protocol complied with the Helsinki Declaration: recommendations guiding physicians in biomedical research involving human subjects. The protocols of the measurements were approved by the National Medical Ethics Committee, Ministry of Health, Republic of Slovenia (Tel: +386 01 478 69 13, http://www.kme-nmec.si/kontakt/, Unique Identifier No. 0120-297/2018/6). Written, informed consent to publish identifying information/images was obtained from the 62-year-old male subject, who was also informed about the purpose and the procedures of the research.

We report on a Caucasian man who presented with angina pectoris, atherosclerosis, hypercholesterolomy, coronary artery disease and subtotal occlusion of the left anterior descending artery. As an immediate intervention in January 2014, coronar angiography, percutaneous implantation of a stent and catheterization/cannulation of the second vein, were performed. Currently, the subject has bradycardia with a HR significantly below 60, coronary artery disease, mild insomnia and autoimmune hypothyroidism.

The activity of the thyroid was assessed in July 2016 using the method of thyroid scanning with radioactive label Technetium 99m. It was shown that Technetium 99m was strongly accumulated in the right lobus, actually delineated region of inflammation, and poorly in the left lobus. A predisposition factor for the development of hypothyroidism in the subject could be excess iodine exposure (i.e., from iodinated-contrast radiographic study) during percutaneous implantation of the stent and catheterization/cannulation of the second vein. The subject also had a history of thyroid disease and was thus at higher risk of iodine-induced hypothyroidism. Since atherosclerosis is a general feature of autoimmune diseases,[34] the current therapy of the subject with autoimmune hypothyroidism also includes cardiovascular aspects: Atoris 10 mg in the evening, Prenessa 4 mg in the morning, Concor 2.5 mg in the evening, Aspirin P 100 life time and Eutirox 100 µm (generic name: Levothyroxine) in the morning. The Aforementioned bradycardia could the result of beta-blocker therapy with Concor.

In the subject, no facial or ear pain, no recent ear trauma and no skin-related contraindications at the site of stimulation, were present. There were also no personal or family history of seizure, mood, dependence on alcohol or recent illicit drug use and pharmacological agents known to increase seizure risk.

The findings of Frangos et al.,[35] provided evidence that in humans, the central projections of the auricular branch of vagus nerve (VN), are consistent with the "classic" central vagal projections and can be accessed non-invasively via the external ear. The proposed idea of selective tANS of the CC belonging to the auricular branch of the VN was developed based on our own reflections and published results.[35,7] In this regard, an area of the CC where supposedly 100 % of innervation belongs to the auricular branch of the VN was assumed.[9,11]

The auricular branch of the VN leaves the cervical VN at the level of the jugular ganglion. The auricular nerve (AN) fibres run between the ear cartilage and the

skin and form a cutaneous receptive field at the external ear that is susceptible to tANS. The AN is composed of myelinated Ab fibres, myelinated Ad fibres and non-myelinated C fibres. The AN endings provide the sensory innervation for specific regions of the external ear, such as the CC,[7,9] and represent a direct gateway to a non-invasive sensory input to the CNS. Since the tANS modulates the parasympathetic auricular branch, various systemic effects on the entire body can be expected.

Figure 1 shows a detailed schematic diagram of the four-channel tANS. **Figure 1** shows the stimulating sites on the CC that were assumed to be relevant for the tANS. They were indicated in the following order: pole position, red (R); below pole position, yellow (Y); above bottom position, black (B); and bottom position, white (W). **Figure 1** also shows parts of the tANS set-up, including an equivalent circuit model (ECM) of the interface at the cathode and anode, parts and the locations of probes of the measuring set-up, hardware parts and the data-acquisition set-up.

The selective tANS proposes the use of a train of mopolar, cathodic-first, current-regulated, biphasic pairs composed of a rectangular cathodic phase (i_c) and anodic phase (i_a).[36] The i_c generates an electric field gradient (driving function) in the skin layers under the cathode, where the receptors, sensory axons and nerve endings are located.[37] To activate most of them, the voltage output of the constant-current stimulator must exceed approximately 30 V, thus overcoming the resistance of the skin layers and delivering the i_c required for the tANS.[38,39] In the anodic phase, the directions of the current phases are reversed. In this case, the anodic phase i_a does not elicit depolarization at the stimulating site, but hyperpolarization. At the same time, the cathodic charge density at the common anode is too low to elicit any stimulation of the muscle tissue below the anode.

Then, they send signals to the spinal cord and the CNS, proposing that the sent signals modulate the autonomic and CNS. As a result, measurable changes in the vital functions of the cardio-vascular system, respiratory system and thyroid elicited with selective tANS of the left and right CC could be expected. It was proposed that in addition to the physiological thermal regulatory and hemodynamic processes within the thyroid, tANS has a noticeable effect on the skin temperature. The time-evolution of the skin temperature during tANS can provide useful information about the adaptation of the thyroid as a function of tANS.[40,41]

The devices that comprised the tANS set-up are the plugs shown in **Figure 2** and the stimulating system

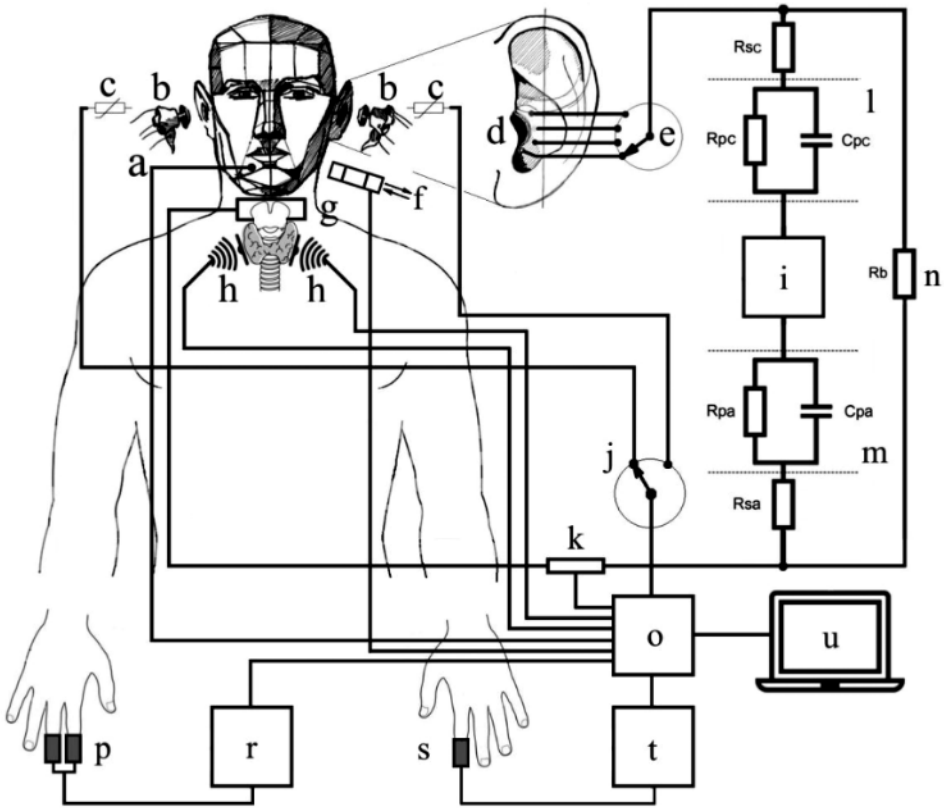

Figure 1: Schematic diagram of the four-channel tANS: (a) body-temperature sensor, (b) plug, (c) BetaCHIP temperature probe, (d) stimulating sites at the CC, (e) switching unit, (f) air-flow sensor, (g) common anode, (h) IR thermometers above the LL and RL of the thyroid, (i) electric stimulator, (j) BetaCHIP temperature probe switching unit, (k) i_c measuring resistor, (l) cathodic interface, (R_{sc}) cathodic serial resistance, (R_{pc}) cathodic parallel resistance, (C_{pc}) cathodic parallel capacitance, (m) anodic interface, (R_{pa}) anodic parallel resistance, (C_{pa}) anodic parallel capacitance, (R_{sa}) anodic serial resistance, (n) (R_b) body resistance, (o) analogue digital adapter, (p) GSR sensor, (r) GSR driver, (s) finger clip SpO2 sensor, (t) pulse oximeter and (u) personal computer

shown in **Figure 3**. **Figure 2a** shows the plug that is the most important part of the system and contains four platinum stimulating electrodes (cathode). The plugs are crafted using commercially available silicone ear plugs that are used by swimmers (Slazenger Ear Plugs, Slazenger Product Code: 885037, United Kingdom). The cathodes are made of 5-mm-long pieces of platinum wire with a diameter of 0.3 mm (99.99 % purity) (Zlatarna Celje d. d., Kersnikova 19, 3000 Celje, Republic of Slovenia). For crafting the cathodes, a portable gas-welding device (Roxy Kit Plus, 3100 °C, Rothenberger Industrial GmbH, Kelkenheim, Germany) with a micro-burner was used. As soon as a piece exposed to the flame begins to melt, the globule begins to form due to the surface energy of the melted platinum. Afterwards, the resulting globular cathodes with a diameter of approximately 1.2 mm shown in **Figure 2b**, were welded to the insulated lead wires using a custom-designed, capacitive-discharge, research spot welder. The obtained geometric surface of an individual cathode to be deployed during tANS was one-half surface of the globule and was of approximately 2.4 mm^2. Subsequently, the cathodes were attached to the pre-defined sites of the silicone plugs and fixed using a silicone adhesive (ASC, Applied Silicone Corporation, Part No: 40064, MED RTV adhesive, implant grade, Santa Paula, California, U.S.A.).

Finally, **Figure 2c** shows the Micro-BetaCHIP (Model GA10K3MCD1, Accuracy ± 0.2°C, Resistance 10 kΩ at 25 °C, Measurement Specialties, Inc., a TE Connectivity Company, Shrewsbury, MA 01545, U.S.A.) temperature probe inserted into each of the silicone plugs that was intended to be used for he measurement of relative temperature variations within the plugs.

The components of the stimulating system are shown **Figure 3**. **Figure 3a** shows an electrical stimulator that was the certified (FDA, Medical CE, FCC, ISO13485) dual-channel microprocessor-controlled device for transcutaneous nerve stimulation with two independent outputs (Model SM9079, Shenzhen L-Domas Technology Ltd., Shenzhen, Guangdong, China). Furthermore, **Figure 3b** shows the dummy headphones with a force applicator to provide an appropriate pressure on the plugs and thus ensure the low impedance $|Z|$ of the interface between the cathodes and the stimulating sites at the CC. By doing so, a more uniform dispersion of the current paths between the cathodes and the stimulating sites is obtained. The force applicator shown in **Figure 3b** is a latex sponge pad mounted on a vice containing soft spring that is mounted into the dummy headphones. During the tANS, each of the plugs is pushed into an external ear at a force of approximately 2.5 N. **Figure 3c** shows the Axelgaard PALS Platinum Neurostimulation Electrode with MultiStick Gel (Model: 895240, Rectangle (2" × 3-1/2"), (5 × 9) cm, AXELGAARD MANUFACTURING CO., LTD., Fallbrook, CA 92028, U.S.A.) common electrode (anode) that was reusable and self-adhering with a geometric surface of about 4500 mm^2. Finally, **Figure 3d** shows the switching unit that was used to select the particular cathode to deliver tANS to the corresponding red, yellow, black or white site at the CC.

The devices that comprised the measuring set-up are shown in **Figure 4**. **Figure 4a** shows the NTC BT sensor (Model JP402, Resistance 10 kΩ at 25 °C, Accuracy 0.5 %, Time to accurate measurement 3 s, J. P. Sensor, Hefei, Anhui, China) used to measure the average of a normal subject's BT using the mouth (oral method).[18] This accurate and stable NTC comply with medical certification (ISO13485). The NTC was connected directly to the high-performance data-acquisition system (DEWE-43, DEWESOFT d. o. o., Republic of Slovenia) according to the instructions of the producer. Afterwards, the NTC was calibrated using a digital fever thermometer (SFT 01/1-Fever Thermometer, Laboratory Accuracy ± 0,1 °C, Sanitas (Sanitas is the brand of Hans Dinlage GmbH), Madrid, Spain).

Figure 4b shows the non-contact IR thermometer (CJMCU-614 (Wuxi Sichiray Co., Ltd., China) used to assess variations of the thyroid temperature.[42] The IR

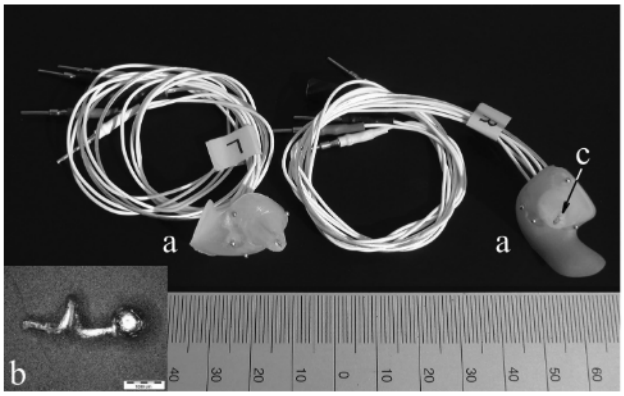

Figure 2: Plugs: a) left and right plug, b) magnified view of an electrode, c) Micro-BetaCHIP temperature probe

Figure 3: Stimulating system: a) electrical stimulator, b) dummy headphones, c) anode and d) switching unit

thermometer uses the Melexis chip (Model: MLX90614 AAA, Resolution 0.02°C, Accuracy ± 0.5 °C at 25 °C, Melexis Technologies NV, Tessenderlo, Belgium) that is a high-accuracy, high-resolution, non-contact thermometer with a 90-degree field of view. The IR thermometer provides digital TTL communications as well as analogue voltage output communication. The analogue output used in the study directly measures the out pin voltage and converts it to the measured temperature (T_m) according to the equation:

$$T_m = A_o / S_v \times 100 = (A_o\ [V]) / (5\ [V]) \times 100 = \\ = A_o \times 20\ [°C] \quad (1)$$

where S_v = 5 V is the supply voltage and A_o is the analogue output in volts.

An IR thermometer was designed to sense IR radiation coming exclusively from the thyroid, excluding any reflected environmental part. To achieve this, an IR sensor was encapsulated to ensure thermal equilibrium and under isothermal conditions to minimize temperature differences across the package that could heat the sensing element in the thermometer and also the thermometer package.

Figure 4c shows the GSR that was used to assess skin conduction, that could potentially be changed during tANS.[43] For this purpose, two silver and silver chloride (Ag/AgCl) electrodes (Biopotential Skin Electrode, E224, IN VIVO METRIC, Healdsburg, California, USA) used as a GSR sensor were attached to an inner surface of the two-finger gloves and connected to the GSR driver. The original electrode was ground so the surface directly touched the skin at the recording site.

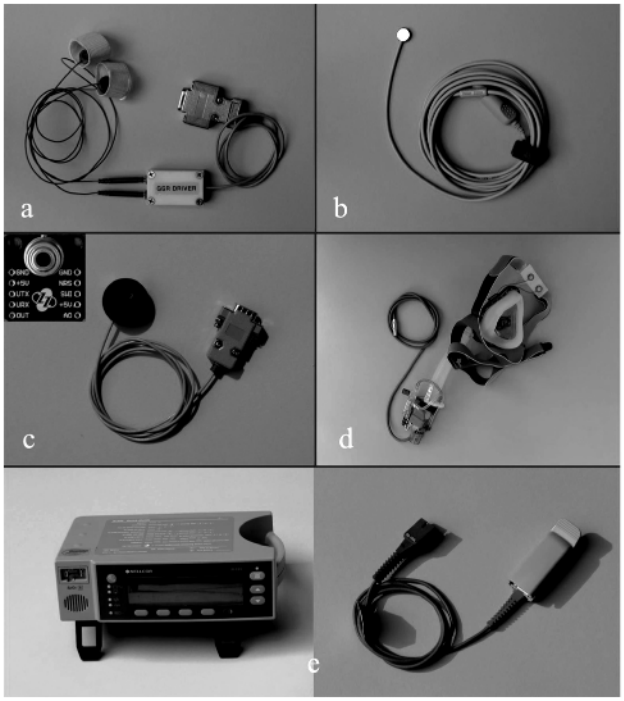

Figure 4: Measurement set-up: a) GSR sensor with driver, b) BT NTC, c) IR thermometer, d) air-flow measuring system, e) pulse oximeter and heart-rate sensory system.

Figure 4d shows the pulse oximeter and heart-rate sensory system that was used to measure SpO2 during the tANS. For this purpose, a pulse oximeter (Nellcor N-595, SpO2 accuracy ± 2 % (90–100 %), ± 3 % (70–89 %), pulse rate accuracy ± 1 bpm (30–90 bpm), 2 bpm (60–149 bpm), 3 bpm (150–245 bpm), Tyco Healthcare Group LP, Nellcor Puritan Bennett Division, Pleasanton, CA, U.S.A.) with a light-based reusable adult finger clip SpO2 sensor (Nellcor DS-100A, Tyco Healthcare Group LP, Nellcor Puritan Bennett Division, Pleasanton, CA, U.S.A.), was used.

Finally, **Figure 4e** shows the air-flow measuring system that was used to assess the variations of the airflow (AF), the changes in the rhythm and the character of the respiration produced by selective tANS. This system comprised a full-face mask with headgear (iVolve Full Face Mask, BMC Medical Co., Ltd., Shijingshan, Beijing, China) and a single-use paediatric/adult ventilator flow sensor (Hamilton 281637 Flow Sensor, (ISO5356-1), Accuracy (± 10 %), Increase resistance <2.5 mbar, Pressure range (± 100 mbar), HAMILTON MEDICAL, Hamilton Medical AG, Bonaduz, Switzerland) that was connected to the full-face mask. The AF sensor actually measured the pressure difference close to the subject's airway elicited by the bi-directional total nasal airflow. To measure this pressure difference, a modified single-use transducer for invasive blood pressure monitoring (DPT-6000, PvB-Critical care, Smiths Medical Deutschland GmbH, Germany) attached to a flow sensor was used. The transducer was re-designed to measure the positive and negative pressure elicited by bi-directional AF and to provide an analogue output signal proportional to the differential pressure. Consequently, in the pressure-flow curve, the horizontal line denotes zero airflow, with negative flow values corresponding to periods of inhalation, and positive flow values corresponding to periods of exhalation.

Prior to subject use, the flow sensor was calibrated with reliable spirometer (Vyntus® SPIRO-USB PC, CE0086, CareFusion, Yorba Linda, CA, U.S.A.) and temperature compensated. During the calibration, the lower limit of the normative unilateral nasal airflow (60 ± 20) mL/s (3.6 ± 1.2) L/min) and upper limit of the normative unilateral airflow (191 ± 20) mL/s (11.46 ± 1.2 L/min), were considered.[30]

Common Experimental Procedures:

- at least 15 minutes were allowed after any workout before taking a measurement,
- consumption of hot or cold food or a beverage, chewing gum, and smoking were prohibited prior to a measurement,
- preparing a subject for recording,
- the subject and the IR thermometers remained at the same ambient temperature (between 23 °C and

Table 1: Mechanical and electrical performance of stimulating electrodes

	Geometric surface	Injected charge	Charge density
Stimulating cathode	A_c = 2.41 mm^2	Q_c = 10 μC	C_d = 4.15 μC/mm^2
Common anode	A_d = 4.500 mm^2	Q_a = 10 μC	A_d = 2.22 nC/mm^2

25 °C) for at least 10 min before oral body and thyroid temperature was assessed.

- the skin at the CC, the skin at the back cervical neck, the skin at the lobes of the thyroid, the skin at the forefinger and at the long finger of the subject was degreased with 70 % isopropyl alcohol and allowed to dry,
- measuring site on the left and right lobes of the thyroid were identified and marked with the sign + using a black felt pen.
- the NTC was placed in the posterior sublingual pocket under the subject's tongue, slightly off centre.
- the subject was instructed to his keep mouth closed and not to bite on the temperature sensor.
- deposition of a thin layer of transparent conductive hypoallergic water-soluble gel (GEL G008, FIAB Spa, Vicchio –Firenze, Italy) onto the CC,
- insertion of plugs into the external ears,
- placing dummy earphones,
- adjusting the force of the plugs while pushed into an external ear using a vice within the dummy headphones,
- placement of the SpO2 sensor on the left forefinger,
- placement of the two Ag/AgCl electrodes on the forefinger and the middle finger of the right nondominal hand,
- placement of the air-flow measuring system on the face,
- placement of the IR thermometers above the left and the right lobes of the thyroid using disposable washers (VHB tape-3M4910, Zhuhai Huayuan Electronics Co., Ltd, Zhuhai City, China),
- measurements performed under the same conditions between 10.15 and 11.15,
- tANS trials were completed with the subject in the sitting position.

The temporal parameters of the rectangular current biphasic stimulating pulse pairs (cathodic and anodic phase) and that of the pulse trains used for the tANS, were selected on a touch screen by the subject and were the following:[44]

- frequency – f = 45.5 Hz (λ = 21.978 ms),
- stimulating phase width – t_c = 200 μs,
- anodic phase width – t_a = 200 μs,
- interphase delay – d = 180 μs,
- on time (pulse train duration) – 2.0 s,
- time gap between successive pulse trains – 1.0 s,
- duty cycle – 3.0 s.

The stimulating intensity i_c however, was pre-set by the subject using a dial on the electrical stimulator until the minimum discomfort at the particular site below the deployed cathode was detected.[45] In the tANS trials, the i_c is assessed continuously by measurement of the voltage drop on the precision serial resistor at the stimulator output.

Considering the current waveform and i_c = 50 mA, which was actually assessed as an optimum in the tANS, the electrical performance of stimulating electrodes were calculated as summarized in **Table 1**.

During 20-minute trials, the tANS was applied via each of the four cathodes of the left and right plugs. Each 20-minute trial started with the 5-minute placebo segment where stimulating pulses were not delivered, proceeded with the 10-minute tANS segment and ended with the 5-minute placebo segment where stimulating pulses were not delivered.

After eight trials in which beta-blocker therapy was used, one of the most indicative sites on the left and one on the right CC were identified. Afterwards, one additional trial one on the left identified and one on the right identified site in which beta-blocker therapy was omitted, were performed.

In the tANS of sites on the left and right CC, the following eight quantities shown in the **Table 2** were measured.

Table 2: Measured quantities

Entity	Acronym	Unit
Stimulating current	i_c	mA
Galvanic skin response	GSR	μS
Body temperature	CT	°C
Temperature of the left thyroid lobe	TLL	°C
Temperature of the right thyroid lobe	TRL	°C
Airflow	AF	m^3/h
SpO2	SpO2	%
Pleth waveform	PLW	A.U.

The assessed eight signals were conditioned and fed to a high-performance data-acquisition system (DEWE-43, DEWESOFT d. o. o., Republic of Slovenia). Afterwards, the data for all eight signals were gathered at 200 kHz using the acquisition software from the same company (DEWESoft 7.0.2). The data was stored on a portable computer (Lenovo W541, Lenovo, Beijing, China).

To evaluate the effect of tANS on the tested vital functions that were induced during 10-minute selective tANS of the left and right CC, each of three segments within a particular recording, i.e., observations before tANS, during tANS and after tANS, were analysed man-

ually using the acquisition software and portable computer.

In an off-line analysis, an average of all the entities calculated within the particular time period are the following:

LBPU [s] – length of BPU was calculated from readings during 25 pulsations,

LBR [s] – breath length was calculated from readings during 10 breaths,

AFBR [m^3/h] – peak-to-peak air flow was calculated from readings during 10 breaths,

SBR [s] – maximum slope of air flow elicited by the mechanism in which the lungs are expanded by elevation of the ribs, was calculated from readings during 10 breaths,

TLL [°C] – temperature of the left lobe was calculated from readings a during 10 breaths,

TRL [°C] – temperature of the right lobe was calculated from readings during 10 breaths,

BT [°C] – body temperature, was calculated from readings during 10 breaths,

GSR [µS] – galvanic skin response was calculated from readings at 10 breaths within the time periods without tANS,

SpO2 [%] – SpO2 was calculated from readings during 10 breaths,

PLWINH [A.U.] – peak-to-peak PLW was calculated from readings for 10 BPU during inhalation,

PLWEXH [A.U.] – peak-to-peak PLW was calculated from readings for 10 BPU during exhalation,

HR [min^{-1}] – heart rate was calculated from readings for 25 BPU,

BR [min^{-1}] – breathing rate was calculated from readings for 10 breaths,

LBPUINH [s] – length of 10 BPU was calculated from readings for 10 inhalations,

LBPUEXH [s] – length of 10 BPU was calculated from readings for 10 exhalations,

DVINH [A.U] – dynamic viscosity at inhalation was calculated as the halved product of the average peak-to-peak PLW and average length of 10 BPU from readings during 10 inhalations,

DVEXH [A.U.] – dynamic viscosity at exhalation was calculated as the halved product of the average peak-to-peak PLW and average length of 10 BPU from readings during 10 exhalations.

Table 3 was constructed to contain six groups of columns/entities describing: experimental conditions, respiratory function, thermal function, physiological arousal, heart function and effect. Each entity was assigned an upward-or downward-coloured arrow representing (↑) the increased positive effect of the tANS, (↓) the decreased positive effect of the tANS, (→) no effect of the

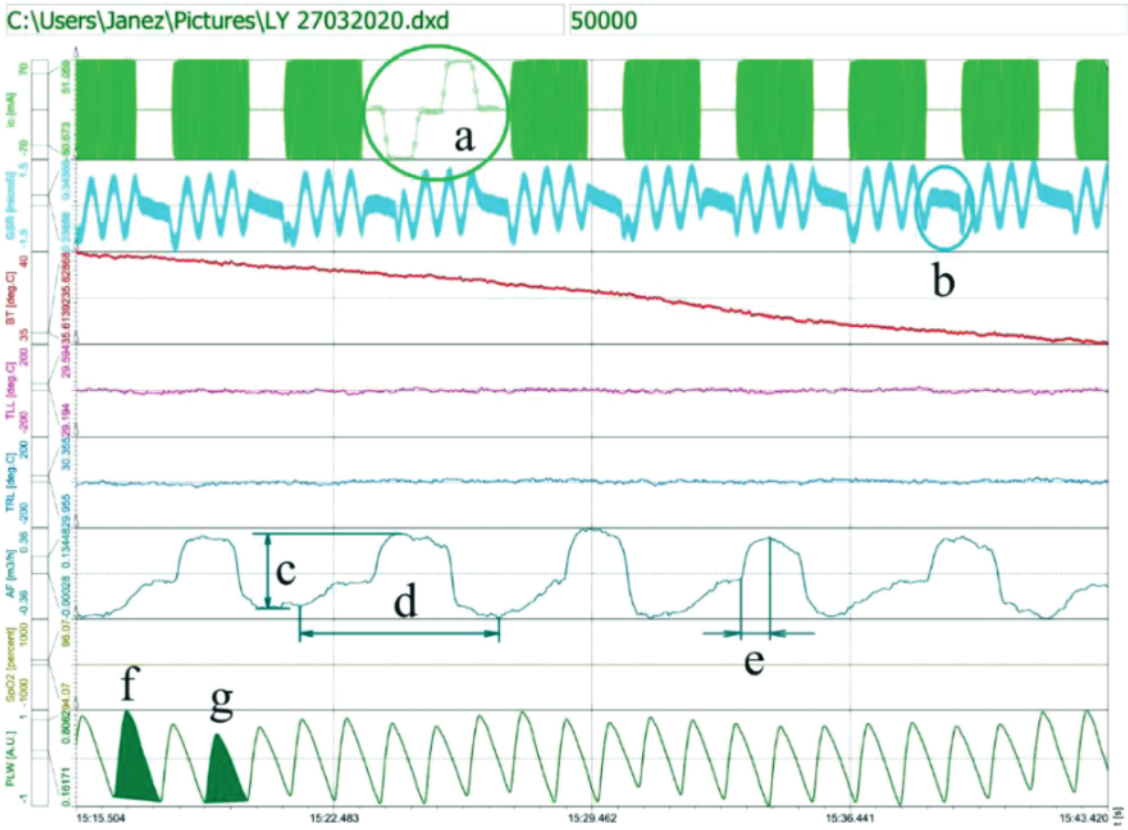

Figure 5: Quantities recorded during selective tANS of LY (from top to bottom): i_c, GSR, BT, TLL, TRL, AF, SpO2 and PLW. Details: a) i_c, b) GSR, c) AFBR, d) LBR, e) SBR, f) DVINH and g) DVEXH.

EXPERIMENTAL CONDITIONS			RESPIRATORY FUNCTION									THERMAL FUNCTION						PHYSIOLOGICAL AROUSAL		HEART FUNCTION				EFFECT	
TRIAL	tANS	i_c [mA]	LBR [s]		SBR [s]		AFBR [m3/h]		BR [min^{-1}]		SpO2 [%]	TLL [°C]		TRL [°C]		BT [°C]		GSR [µS]		HR [min^{-1}]		DVINS [A.U.]		DVEXP [A.U.]		TOTAL SCORE	
																									Σ	Σ
LR	LP	NA	4,38		0,89		0,433		13,00		95,08	28,9		30,6		36,53		0,319		47,0		0,279		0,236			
	LR	51,6	4,14	↓	0,85	↓	0,457	↑	15,60	↑	96,24	28,9	↕	30,6	↕	36,55	↑	0,307	↓	53,1	↑	0,324	↑	0,294	↑	3	7
	LP	NA	4,62	↑	1,27	↑	0,457	↑	13,10	↑	95,08	28,9	↕	30,6	↕	36,51	↑	0,307	↓	53,6	↑	0,273	↓	0,236	↕	5	3
LY	LP	NA	5,58		1,10		0,431		10,20		96,23	29,4		30,2		35,64		0,347		49,9		0,528		0,449			
	LY	50,6	5,12	↓	0,73	↓	0,450	↑	11,56	↑	95,07	29,4	↕	30,2	↕	35,63	↓	0,350	↑	50,8	↑	0,335	↓	0,291	↓	6	4
	LP	NA	4,65	↓	0,51	↓	0,398	↓	13,00	↑	95,07	29,4	↕	30,2	↕	35,47	↓	0,356	↑	49,4	↓	0,366	↓	0,311	↓	6	4
LB	LP	NA	4,76		0,71		0,447		12,27		96,62	27,4		29,9		35,67		0,361		48,2		0,258		0,214			
	LB	46,4	5,39	↑	0,95	↑	0,471	↑	11,03	↓	97,61	27,4	↕	29,9	↕	36,05	↑	0,348	↓	49,3	↑	0,300	↑	0,260	↑	4	6
	LP	NA	5,50	↑	0,78	↑	0,452	↑	10,80	↓	97,01	27,4	↕	29,9	↕	36,11	↑	0,352	↓	49,2	↑	0,317	↑	0,272	↑	4	6
LW	LP	NA	4,24		0,59		0,437		11,54		95,06	29,2		30,3		36,05		0,331		48,6		0,296		0,244			
	LW	49,6	4,90	↑	0,46	↓	0,440	↑	12,00	↑	95,06	29,2	↕	30,3	↕	36,06	↑	0,329	↓	48,7	↑	0,397	↑	0,374	↑	3	6
	LP	NA	4,80	↑	0,58	↓	0,481	↑	12,45	↑	95,76	29,2	↕	30,3	↕	36,10	↑	0,330	↓	50,4	↑	0,397	↑	0,369	↑	4	6
RR	RP	NA	4,44		0,47		0,442		13,49		96,23	29,7		29,9		35,75		0,308		52,3		0,279		0,239			
	RR	51,5	4,52	↑	0,55	↑	0,481	↑	13,27	↓	96,23	29,7	↕	29,9	↕	35,99	↑	0,311	↑	51,6	↓	0,279	↕	0,225	↓	6	2
	RP	NA	5,41	↑	0,78	↑	0,468	↑	11,12	↓	96,11	29,7	↕	29,9	↕	36,20	↑	0,308	↕	51,3	↓	0,279	↕	0,231	↓	5	3
RY	RP	NA	5,23		0,89		0,459		11,51		96,23	29,8		30,3		35,94		0,328		49,6		0,290		0,235			
	RY	51,3	4,33	↓	0,81	↓	0,546	↑	13,50	↑	96,23	29,7	↓	30,2	↓	36,07	↑	0,323	↓	49,7	↑	0,278	↓	0,225	↓	4	6
	RP	NA	4,35	↓	0,58	↓	0,430	↓	13,45	↑	96,23	29,8	↕	30,2	↓	36,17	↑	0,322	↓	51,5	↑	0,272	↓	0,218	↓	3	7
RB	RP	NA	5,02		0,48		0,448		11,79		96,23	29,1		30,0		35,52		0,330		52,0		0,265		0,233			
	RB	48,2	4,88	↓	0,58	↑	0,548	↑	12,26	↑	96,31	29,2	↕	30,0	↕	35,57	↑	0,312	↓	49,5	↑	0,322	↑	0,263	↑	5	5
	RP	NA	5,34	↑	0,60	↑	0,514	↑	11,27	↓	96,23	29,2	↕	30,0	↕	35,74	↑	0,319	↓	49,6	↑	0,370	↑	0,315	↑	4	5
RW	RP	NA	5,66		0,69		0,450		10,62		96,32	27,4		27,6		35,45		0,350		48,9		0,283		0,249			
	RW	51,7	4,83	↓	0,64	↓	0,500	↑	12,64	↑	96,01	27,5	↕	27,6	↕	35,61	↑	0,327	↓	49,1	↑	0,286	↑	0,244	↓	3	7
	RP	NA	6,14	↑	0,93	↑	0,539	↑	10,09	↓	96,24	27,5	↕	27,6	↕	35,68	↑	0,336	↓	52,4	↑	0,268	↓	0,228	↓	5	5
LY*	LP	NA	5,33		0,70		0,436		11,16		95,08	27,4		27,0		36,74		0,290		65,1		0,206		0,190			
	LY*	51,8	4,28	↓	0,56	↓	0,482	↑	13,93	↑	95,09	27,4	↕	27,0	↕	36,64	↓	0,292	↓	66,2	↑	0,262	↑	0,241	↑	5	5
	LP	NA	4,92	↓	0,67	↓	0,422	↓	12,20	↑	94,69	27,4	↕	27,1	↑	36,56	↓	0,287	↓	65,2	↑	0,201	↓	0,180	↓	5	6
RR*	RP	NA	5,54		0,63		0,446		10,89		95,66	26,0	↕	28,4		36,74		0,314		69,2		0,194		0,179			
	RR*	52,3	4,56	↓	0,53	↓	0,425	↓	13,06	↑	95,31	26,0	↕	28,3	↓	36,21	↓	0,311	↓	71,3	↑	0,188	↓	0,168	↓	4	7
	RP	NA	4,63	↑	0,51	↓	0,468	↑	12,94	↑	95,08	26,0	↕	28,4	↕	36,14	↓	0,315	↑	69,5	↑	0,209	↑	0,168	↓	6	4

Table 3: Averaged results of the analysis of the effects of selective tANS on the left and right CC.

Legend:
LP – Left placebo
LR – Left red
LY – Left yellow
LB – Left black
LW – Left white
RP – Right placebo
RR – Right red
RY – Right yellow
RB – Right black
RW – Right white
i_c [mA] – Stimulating current
LBPU [s] – Length of 25 BPU (increase means positive effect),
LBR [s] – Length of 10 Breaths (increase means positive effect),
AFBR [m^3/h] – Peak-to-peak air flow of 10 breaths (increase means positive effect),
SBR [s] – Maximum slope of 10 breaths (increase means positive effect),
TLL [°C] – Temperature of left lobe (increase means positive effect),
TRL [°C] – Temperature of right lobe (increase means positive effect),
BT [°C] – Body temperature (increase means negative effect),
GSR [µS] – Galvanic skin response (increase means positive effect),
SpO2 [%] – SpO2 during 10 breaths (increase means positive effect),
PLWINH [A.U.] – Peak-to-peak PLW of 10 BPU during inhalation (increase means negative effect),
PLWEXH [A.U.] – Peak-to-peak PLW of 10 BPU during exhalation (increase means negative effect),
HR [min^{-1}] – Heart rate (increase means negative effect),
BR [min^{-1}] – Breathing Rate (increase means positive effect),
LBPUINH [s] – Length of 10 BPU during inhalation (increase means negative effect),
LBPUEXH [s] – Length of 10 BPU during exhalation (increase means negative effect),
DVINH [A.U] – Dynamic viscosity during 10 inhalations (increase means negative effect),
DVEXH [A.U.] – Dynamic viscosity during 10 exhalations (increase means negative effect).
↑ – Increased positive effect of the tANS.
↓ – Decreased positive effect of the tANS.
↕ – No effect of the tANS.
↑ – Increased negative effect of the tANS.
↓ – Decreased negative effect of the tANS.
Σ – Score of positive effects.
Σ – Score of negative effects.
* – Trial without beta-blocker therapy.

tANS, (↑) the increased negative effect of the tANS and (↓) the decreased negative effect of the tANS, respectively. Afterwards, the positive and negative effects of trials depicted in **Table 3** were assigned with the corresponding score.

On the basis of the total score in **Table 3**, the most indicative site LY on the left and the most indicative site RR on the right CC, were identified for the two additional tANS trials in which beta-blocker therapy was omitted.

To graphically represent the overall effects of selective tANS for the left and right CC on the respiratory function, thermal function, physiological arousal and heart function, **Figure 6** was constructed, considering positive and negative effects depicted in **Table 3**. Both, **Table 3** and **Figure 6**, were constructed on the basis of 1770 readings taken manually from recordings of the ten trials and 520 calculations.

Regarding statistical analyses, only average values of ten and twenty-five readings obtained from each of the

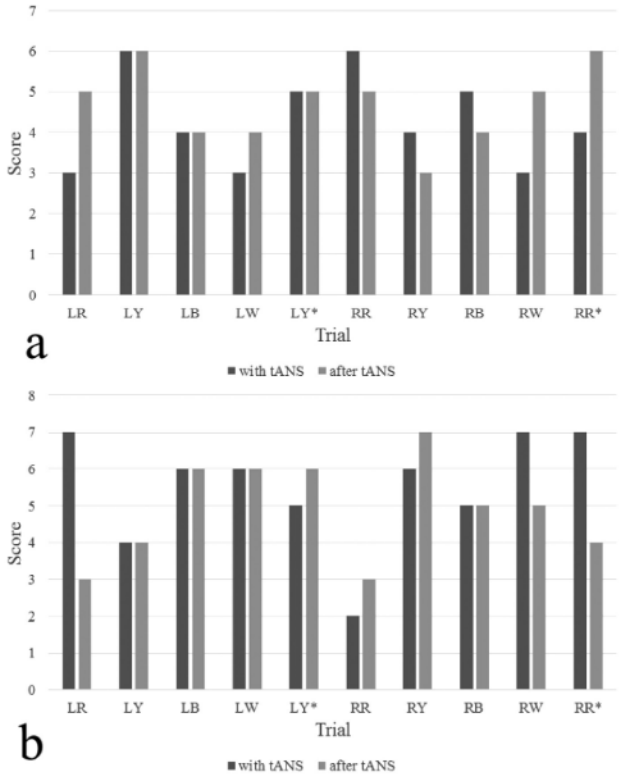

Figure 6: Score of the effects of selective tANS for the left and right CC: a) Positive effects, b) Negative effects

ten recordings, could be calculated. To present any reliable statistical analysis, the number of readings obtained was too small.

3 RESULTS

Figure 5 shows an example of the responses of the respiratory function, thermal function, physiological arousal and heart function, measured during selective tANS at the site LY on the left CC. It is a trace of i_c, GSR, BT, TLL, TRL, AF, SpO2 and PLW, recorded over an interval spanning five breaths during the selective tANS of LY. Detail (**a**) in **Figure 5** shows a stimulating current (i_c), detail (**b**) shows an interval between stimulating trains where the actual value of the GSR was measured, detail (**c**) shows the AFBR, detail (**d**) shows the LBR, detail (**e**) shows the SBR, detail (**f**) shows the DVINH and detail (**g**) shows the DVEXH.

Table 3 contains the averaged results of an analysis of the effects obtained from selective tANS of the left and right CC on the respiratory function, thermal function, physiological arousal and heart function, as well as the assigned score.

Figure 6 shows the overall score and the ratio of positive and negative effects of the selective tANS fot the left and right CC on the respiratory function, thermal function, physiological arousal and heart function.

4 DISCUSSION

In this study we evaluated the effects of selective tANS at predefined sites for both CC on certain vital functions, i.e., the respiratory function, thermal function, physiological arousal and heart function, of a 62-year-old patient with stable angina pectoris 6 years after an acute myocardial infarction. The objectives were to test the selectivity of tANS and to identify, record and analyse the short-term responses of the cardio-vascular system, the respiratory system and the thyroid. The idea of using selective tANS was based on anatomical evidence showing that the outer ear is the only place on the surface of the human body where the afferent vagus nerve distribution can be transcutaneously stimulated.[7,45] We presumed that the i_c spreading from the cathode could activate a certain population of nerve endings within a specific volume of the CC. Namely, the applied cathodic charge density $C_d = 4.15$ μC/mm^2 is sufficient to stimulate the subcutaneous neural structures of the CC, while the anodic charge density $A_d = 2.22$ nC/mm^2 is too low to elicit any stimulating effect in the neck muscles. To the best of our knowledge there have been no studies on the effects of tANS on thyroid blood flow based on measurements of skin temperature using two IR thermometers.

The overall hypothesis of the study was that the selective tANS of predefined sites on the left and right CC can have a measurable effect on some vital functions in patients with angina pectoris. As demonstrated by the total score shown in **Table 3** and the ratio between the positive and negative effects shown in **Figure 6**, the most significant effect averaged for all the tested vital functions was observed in the trials RR and LY, with a less significant one in the trials LW and RY. In other trials, these effects were found to be between the above two results. Accordingly, this hypothesis was confirmed.

The first specific hypothesis was that the selective tANS has a measurable effect on the respiratory function, which can be expressed as a change in BR, LBR, AFBR, SBR and SpO2. **Table 3** shows that the selective tANS had either a positive or negative effect on the respiratory function in all the trials. An example of the airflow signal elicited by the bi-directional total nasal airflow during a breath is shown in **Figure 5**. It was found that the highest positive and the lowest negative effects were observed in the trial LB, while the lowest positive and highest negative effects were observed in the trial LY. In other trials, these effects were found to be between the above two results. Accordingly, this hypothesis was confirmed.

The second hypothesis, that the interaction between the autonomic nervous system and the rich lymphatic system of the thyroid[19] can be modified with tANS and highlighted with measurements of subtle variations in TLL and TRL for the lobes of the thyroid, was partially confirmed. **Table 3** shows that TLL and TRL measured

for both lobes of the thyroid during all the tANS trials remained unchanged, except in LY*, where TRL was slightly increased, while in RY and RR they were slightly reduced. In short, tANS had a small effect on the blood flow in the thyroid in all the other trials.

The third hypothesis, that tANS can have a positive effect on physiological arousal was confirmed in the trial LY and partly confirmed in the trials RR, LY* and RR*. **Table 3** shows that the GSR in the above-mentioned trials increased with the tANS. Therefore, tANS contributes to the sweat-induced skin wetness.

The final hypothesis that the heart function can be modified with the tANS was confirmed. **Table 3** shows that the highest positive and the lowest negative effects were observed in the trial LY and RR, while the lowest positive and highest negative effects were observed in the trials LB and LW, respectively. In other trials, these effects were found to be between the above two results.

The main difference between our study and the earlier studies of others is that in our study the tANS was delivered selectively to four particular sites on the CC that are believed to be innervated predominantly by the auricular branch of the vagus nerve.[7] One advantage that emerged from the study was deployment of a four-electrode silicone plug, which enabled both selective tANS of the CC and repositioning of the stimulated sites without the need to change the location of the physical electrode. Regarding this, there are still a lot of possibilities to determine better stimulating sites.[46] A limitation of the tested tANS is the vast parameter space, which is closely related to the temporal conditions, the stimulating conditions via the impedance of the stimulating electrodes, the environmental conditions via the temperature and the experimental conditions.

The greatest weakness of the approach was that the stimulating efficiency was dependent on the pressure applied to the plug and thus to the platinum cathodes. As a result, special attention was focused on the requirement that, during the tANS, good cathode-skin contact was made, ensuring that high i_c density peaks were avoided and the stimulation voltage required to drive the stimulator was reduced.[6] By doing so, skin irritation or redness (as the most common side effects of tANS) were avoided.

All the measurements were performed under the same conditions. However, all the trials were carried out by a single researcher, which could have led to some biases.

The AFBR trajectory shown in **Figure 5** can be described using the mechanics of pulmonary ventilation. Inspiration was achieved by a mechanism in which the contraction of the diaphragm pulls the lower surfaces of the lungs downwards, so the chest cavity is shortened, and by a mechanism in which the lungs are expanded by the raising of the ribs so the anteroposterior diameter of the chest cavity is increased. The latter mechanism was validated by SBR, which significantly increased in the trials LB, RR and RB. Expiration, however, can be described by a mechanism in which the diaphragm relaxes, and the elastic recoil of the lungs, chest wall and abdominal structures, compresses the lungs to expel the air.

In all trials before tANS, the BT was lower than that in the heart due to the temperature loss of the blood in its path from the heart towards the forehead. Similarly, the TLL and TRL measured before the tANS were significantly lower than the BT due to the temperature loss of the blood in its path from the heart towards the thyroid. The BT measured during and after the tANS increased in the trials LR, LB, LW, RR, RY, RB and RW, while in the trials LY* and RR* it slightly decreased. The reason for the partial confirmation of the hypothesis regarding TRL and TRL can be found in the very small sensing area of the IR thermometer Φ (3.5±0.1) mm compared to an area of the lobe, so the most relevant site could easily be missed. A possible solution would be a more accurate positioning of the IR thermometer, supported by ultrasound.

It was observed that the time constant of the Micro-BetaCHIP temperature probe that was inserted into the bulky silicone plug was almost 5 min. Therefore, measurements of the relative temperature variations within the CC via the plugs, were not completed.

The average of the GSR in each of the three periods of the particular trial was calculated from readings during the peak inhalation airflow of 10 breaths within an interval between stimulating trains to avoid any interference with the stimuli. The starting value of the GSR in each trial depended on the actual electrical conductance of the skin.

Even though such a negative chronotropic could be expected, it was not the case, presumably due to the medicine, i.e., Concor, prescribed to the patient that contains an active substance called bisoprolol belonging to the group of beta blockers. In trials without the beta-blocker medication, the dose was halved for two days before the final discontinuation to avoid any possible rebound effect, which can occur in the case of abrupt discontinuation. **Table 3** shows that after the first day of the discontinuation of the beta-blocker medication, the HR increased by ten beats and after the second day by another ten beats.

PLW, which is the pattern of the waveform of beat-to-beat changes in stroke volume, can also resemble an arterial pressure waveform and graphically displays the real-time HR. In other words, the pulse pressure is determined approximately by the ratio of the stroke volume output to the compliance of the arterial tree. It was expected that in this elderly subject, the pulse pressure would rise above the normal, because the arteries will have become hardened with arteriosclerosis and, therefore, became relatively noncompliant. It was observed that in all the recorded pletismographs, Dicrotic Notch was not present within the pletismographic pulses. One possible explanation for this could be the prescribed

beta-blocker therapy with Concor that caused the heart to beat more slowly and with less force, which lowers the BP. In contrast, in the recordings of trials without the beta-blocker therapy, Dicrotic Notch was noticed.

The PLW and LBPU that were monitored by the pulse oximeter and recorded were analysed separately during inhalations and exhalations. The resulting entity was calculated as a halved product of the PLW, and the LBPU of the BPU actually represented the area under the particular PLW. This entity, usually expressed in newton second per square metre (Ns/m^2), was actually the dynamic viscosity. Since the pulse oximeter only visualized the blood-volume change in the tissue caused by the passage of blood without a numerical value of the BPU, the resulting dynamic viscosity was expressed in arbitrary units. Accordingly, the DVINH was calculated as the halved product of PLWINH and the LBPUINH of 10 BPU during 10 inhalations, while the DVEXP was calculated as the halved product of PLWEXH and the LBPUEXH of 10 BPU during 10 exhalations.

However, for a more detailed analysis of the tANS effects, computational models incorporating experimental insights will be necessary. The directions of our future work will include tANS at even more sites on the CC with fine tuning of the stimulation parameters, to improve the stimulating electrode-skin contact, to modulate the secretion of hormones, to modulate the heart and respiratory functions, to modulate the function of the thyroid gland and to evaluate the interaction of ventilation and circulation.

Previous studies have indicated that the range of possible applications for selective tANS are vast. For instance, tANS could serve as a promising treatment for neuropsychiatric disorders such as depression and epilepsy. Other studies have demonstrated that tANS can also help in rehabilitation training to restore or accelerate the learning of behaviour,[47] decrease the inflammatory response,[48,49] and can potentially enhance performance and the autonomic function.[50,51]

5 CONCLUSIONS

Given the epidemiological situation and economic and social burdens, the possibility of modulating thyroid secretion by the selective tANS of specific sites on the CC may represent a tremendous breakthrough in the treatment of thyroid disorders.

In the case of using an even more selective tANS with an increased number of channels, this study has the potential to extend the application of tANS to other disorders, such as epilepsy, bipolar disorder, morbidity, jet lag, insomnia, shift-work disorder, circadian rhythm disorders, as well as benzodiazepine and nicotine withdrawal.

Acknowledgment

Research was supported by funding from the Slovenian Research Agency, Ministry of Education, Science and Sport, Ljubljana, Republic of Slovenia, Grant Number P3-0171, which was awarded to the Institute of Pathophysiology, Faculty of Medicine, University of Ljubljana, Ljubljana, Republic of Slovenia.

6 REFERENCES

[1] A. P. Amar, M. L. Levy, C. Y. Liu, M. L .J. Apuzzo, Vagus nerve stimulation, Neuromodulation, Academic Press, London 2009, 625–37

[2] G. M. De Ferrari, P. J. Schwartz, Vagus nerve stimulation: from pre-clinical to clinical application: challenges and future directions, Heart Fail Rev., 16 (**2011**), 195–203, doi:10.1007/s10741-010-9216-0

[3] R. H. Howland, Vagus Nerve Stimulation, Curr. Behav. Neurosci. Rep., 1 (**2014**) 2, 64–73, doi:10.1007/s40473-014-0010-5

[4] R. M. McAllen, K. M. Spyer, Two types of vagal preganglionic motoneurones projecting to the heart and lungs, J. Physiol., 282 (**1978**), 353–364, doi:10.1113/jphysiol.1978.sp012468

[5] J. Ellrich, Transcutaneous vagus nerve stimulation, Eur. Neurol. Rev., 6 (**2011**) 4, 254–6, doi:10.17925/ENR.2011.06.04.254

[6] B. W. Badran, A. B. Yu, D. Adair, G. Mappin, W. H. DeVries, D. D. Jenkins, M. S. George, M. Bikson, Laboratory Administration of Transcutaneous Auricular Vagus Nerve Stimulation (taVNS): Technique, Targeting, and Considerations, J. Vis. Exp., 143 (**2019**), e58984, https://doi.org/10.3791/58984

[7] E. T. Peuker, T. J. Filler, The nerve supply of the human auricle, Clin. Anat., 15 (**2002**) 1, 35–7, doi:10.1002/ca.1089

[8] P. Nogier, R. Nogier, The man in the ear, Maisonneuve, 1985

[9] W. He, X. Wang, H. Shi, H. Shang, L. Li, X. Jing, B. Zhu, Auricular Acupuncture and Vagal Regulation, Evid. Based Complement. Alternat. Med., (**2012**), 786839, doi:10.1155/2012/786839

[10] S. Dietrich, J. Smith, C. Scherzinger, K. Hofmann-Preiß, T. Freitag, A. Eisenkolb, R. Ringler, A novel transcutaneous vagus nerve stimulation leads to brainstem and cerebral activations measured by functional MRI, Biomed. Tech. Biomed. Eng., 53 (**2008**) 3, 104–11, doi:10.1515/BMT.2008.022

[11] M. F. Butt, A. Albusoda, A. D. Farmer, Q. Aziz, The anatomical basis for transcutaneous auricular vagus nerve stimulation, Journal of Anatomy, 236 (**2020**) 4, 588 – 611, doi:10.1111/joa.13122

[12] A. J. E. Bach, I. B. Stewart, A. E. Disher, J. T. Costello, A comparison between conductive and infrared devices for measuring mean skin temperature at rest, during exercise in the heat, and recovery, PLoS ONE, 10 (**2015**) 2, e0117907, doi:10.1371/journal.pone.0117907

[13] R. C. Webb, A. P. Bonifas, A. Behnaz, Y. Zhang, K. J. Yu, H. Cheng, M. Shi, Z. Bian, Z. Liu, Y.-S. Kim, W.-H. Yeo, J. S. Park, J. Song, Y. Li, Y. Huang, A. M. Gorbach, J. A. Rogers, Ultrathin conformal devices for precise and continuous thermal characterization of human skin, Nat. Mater., 12 (**2013**), 938–944, doi:10.1038/nmat3755

[14] V. Bernard, E. Staffa, V. Mornstein, A. Bourek, Infrared camera assessment of skin surface temperature – effect of emissivity, Phys. Medica, 29 (**2013**), 583–591, doi:10.1016/j.ejmp.2012.09.003

[15] B. A. MacRae, S. Annaheim, C. M. Spengler, R. M. Rossi, Skin Temperature Measurement Using Contact Thermometry: A Systematic Review of Setup Variables and Their Effects on Measured Values, Front. Physiol., 9 (**2018**) 29, doi:10.3389/fphys.2018.00029

[16] V. V. Yakovlev, B. A. Utekhin, Errors in skin temperature measurements due to changes in evaporation under the sensor, Bull. Exp. Biol. Med., 60 (**1965**), 1210–1212, doi:10.1007/BF00793268

[17] B. Hapke, Theory of Reflectance and Emittance Spectroscopy: Reflectance spectroscopy, Cambridge University Press, Cambridge 2012, doi:10.1017/CBO9781139025683

[18] Medical News Today, https://www.medicalnewstoday.com/articles/323819 (**2020**)

[19] R. Lenhardt, D. I. Sessler, Estimation of mean-body temperature from mean-skin and core temperature, Anesthesiology, 105 (2006), 1117–1121, doi:10.1097/00000542-200612000-00011

[20] R. O'Rahilly, F. Müller, S. Carpenter, R. Swenson, Chapter 50-The neck, Thyroid glands. in Basic human anatomy (ed. Swenson, R.) (Dartmouth Medical School, 2008). https://www.dartmouth.edu/~humananatomy/part_8/chapter_50.html

[21] A. Leung, Thyroid Emergencies, J. Infus. Nurs., 39 (**2016**) 5, 281–286, doi:10.1097/NAN.0000000000000186

[22] H. Whiteman, How body temperature is affected by thyroid hormone, Medical News Today https://www.medicalnewstoday.com/articles/266255.php (2013)

[23] M. A. Aweda, A. O. Adeyomoye, G. A. Abe, Thermographic analysis of thyroid diseases at the Lagos university teaching hospital, Nigeria, Adv. Appl. Sci. Res., 3 (**2012**) 4, 2027–2032

[24] W. J. Cunliffe, The innervation of the thyroid gland, Acta Anat., 46 (**1961**), 135-141, doi:10.1159/000141776

[25] H. Hotta, A. Onda, H. Suzuki, P. Milliken, A. Sridhar, Modulation of Calcitonin, Parathyroid Hormone, and Thyroid Hormone Secretion by Electrical Stimulation of Sympathetic and Parasympathetic Nerves in Anesthetized Rats, Front. Neurosci., 11 (**2017**), 375, doi:10.3389/fnins.2017.00375

[26] J. Ishii, K. Shizume, S. Okinaka, Effect of stimulation of the vagus nerve on the thyroidal release of 131i-labeled hormones, Endocrinology, 82 (**1968**), 7–16, doi:10.1210/endo-82-1-7

[27] H. Huang, S. Liang, Acupuncture at otoacupoint heart for treatment of vascular hypertension, J. Tradit. Chin. Med., 12 (**1992**) 2, 133–6

[28] A. Jubran, Pulse oximetry, Crit Care., 19 (**2015**) 1, 272, doi:10.1186/s13054-015-0984-8

[29] R. Eccles, Nasal Airflow in Health and Disease, Acta Oto-Laryngologica, 120 (**2000**) 5, 580–595, doi:10.1080/000164800750000388

[30] A. A. T. Borojeni, G. J. M. Garcia, M. Gh. Moghaddam, D. O. Frank-Ito, J. S. Kimbell, P. W. Laud, L. J. Koenig, J. S. Rhee. Normative ranges of nasal airflow variables in healthy adults, Int. J. Comput. Assist. Radiol. Surg., 15 (**2020**) 1, 87–98, doi:10.1007/s11548-019-02023-y

[31] J. Corey, J. Pallanch, Evaluation of Nasal Breathing Function with Objective Airway Testing, Cummings Otolaryngology-Head and Neck Surgery, Elsevier/Mosby, Maryland Heights 2010, 640–656, doi:10.1016/B978-0-323-05283-2.00043-4

[32] D. R. Merrill, The electrochemistry of charge injection at the electrode/tissue interface, Implantable Neural Prostheses 2, Springer, New York 2010, 85–138, doi:10.1007/978-0-387-98120-8_4

[33] C. J. Tyler, The effect of skin thermistor fixation method on weighted mean skin temperature, Physiol. Meas., 32 (**2011**) 10, 1541–1547, doi:10.1088/0967-3334/32/10/003

[34] J. Frostegård, Atherosclerosis in Patients With Autoimmune Disorders. Arteriosclerosis, Thrombosis, and Vascular Biology, 25 (**2005**), 1776–1785, doi:10.1161/01.ATV.0000174800.78362.ec

[35] E. Frangos, J. Ellrich, B. R. Komisaruk, Non-invasive access to the vagus nerve central projections via electrical stimulation of the external ear: fMRI evidence in humans, Brain Stimul., 8 (**2015**) 3, 624–36, doi:10.1016/j.brs.2014.11.018

[36] A. Kuhn, Modeling transcutaneous electrical stimulation, Diss. ETH No. 17948, ETH Zurich, Zurich 2008, 211

[37] E. J. Peterson, O. Izad, D. J. Tyler, Predicting myelinated axon activation using spatial characteristics of the extracellular field, J. Neural. Eng., 8 (**2011**) 4, 046030, doi:10.1088/1741-2560/8/4/046030

[38] Y. A. Chizmadzhev, A. V. Indenbom, P. I. Kuzmin, S. V. Galichenko, J. C. Weaver, R. O. Potts, Electrical properties of skin at moderate voltages: contribution of appendageal macropores, Biophys. J., 74 (2Pt 1) (**1998**) 843–56, doi:10.1016/S0006-3495(98)74008-1

[39] P. M. Elias, Epidermal lipids, barrier function, and desquamation, J. Invest. Dermatol., 80 (**1983**) 1, 44s–9s, doi:10.1038/jid.1983.12

[40] B. B. Lahiri, S. Bagavathiappan, T. Jayakumar, J. Philip, Medical applications of infrared thermography: A review, Infrared Phys. Technol., 55 (**2012**) 4, 221–235, doi:10.1016/j.infrared.2012.03.007

[41] I. Fernández-Cuevas, J. C. B. Marins, J. A. Lastras, P. M. G. Carmona, S. P. Cano, M. Á. García-Concepción. M. Sillero-Quintana, Classification of factors influencing the use of infrared thermography in humans: A review, Infrared Phys. Technol., 71 (**2015**), 28–55, doi:10.1016/j.infrared.2015.02.007

[42] S. Asadian, A. Khatony, G. Moradi, A. Abdi, M. Rezaei, Accuracy and precision of four common peripheral temperature measurement methods in intensive care patients, Med. Devices (Auckl), 9 (**2016**), 301–308, doi:10.2147/MDER.S109904

[43] D. Filingeri, D. Fournet, S. Hodder, G. Havenith, Tactile cues significantly modulate the perception of sweat-induced skin wetness independently of the level of physical skin wetness, J. Neurophysiol., 113 (**2015**) 10, 3462–3473, doi:10.1152/jn.00141.2015

[44] J. Rozman, P. Pečlin, I. Kneževič, T. Mirkovič, B. Geršak, M. Podbregar, Heart function influenced by selective mid-cervical left vagus nerve stimulation in a human case study, Hypertension research, 32 (**2009**) 11, 1041–1043, doi:10.1038/hr.2009.140

[45] T. R. Henry, Therapeutic mechanisms of vagus nerve stimulation, Neurology, 59 (**2002**) 6 Suppl 4, S3–S14, doi:10.1212/wnl.59.6_suppl_4.s3

[46] B. W. Badran, J. C. Brown, L. T. Dowdle, O. J. Mithoefer, N. T. LaBate, J. Coatsworth, W. H. DeVries, C. W. Austelle, L. M. McTeague, A. Yu, M. Bikson, D. D. Jenkins, M. S. George, Tragus or cymba conchae? Investigating the anatomical foundation of transcutaneous auricular vagus nerve stimulation (taVNS), Brain Stimul., 11 (**2018**) 4, 947–948, doi:10.1016/j.brs.2018.06.003

[47] B. W. Badran, D. D. Jenkins, D. Cook, S. Thompson, M. Dancy, W. H. DeVries, G. Mappin, P. Summers, M. Bikson, M. S. George, Transcutaneous auricular vagus nerve stimulation (taVNS) for improving oromotor function in newborns, Brain Stimul., 11 (**2018**) 5, 1198–1200, doi:10.1016/j.brs.2018.06.009

[48] L. V. Borovikova, S. Ivanova, M. Zhang, H. Yang, G. I. Botchkina, L. R. Watkins, H. Wang, N. Abumrad, J. W. Eaton, K. J. Tracey, Vagus nerve stimulation attenuates the systemic inflammatory response to endotoxin, Nature, 405 (**2000**) 6785), 458–62, doi:10.1038/35013070

[49] L. Ulloa, The vagus nerve and the nicotinic anti-inflammatory pathway, Nature Reviews Drug Discovery,4 (**2005**) 8, 673–684, doi:10.1038/nrd1797

[50] B. W. Badran, O. J. Mithoefer, C. E. Summer, N. T. LaBate, C. E. Glusman, A. W. Badran, W. H. DeVries, P. M. Summers, C. W. Austelle, L. M. McTeague, J. J. Borckardt, M. S. George, Short trains of transcutaneous auricular vagus nerve stimulation (taVNS) have parameter-specific effects on heart rate, Brain Stimul., 11 (**2018**) 4, 699–708, doi:10.1016/j.brs.2018.04.004

[51] J. A. Clancy, D. A. Mary, K. K. Witte, J. P. Greenwood, S. A. Deuchars, J. Deuchars, Non-invasive vagus nerve stimulation in healthy humans reduces sympathetic nerve activity, Brain Stimul., 7 (**2014**) 6, 871–7, doi:10.1016/j.brs.2014.07.031